Nuclear Instruments and Methods in Physics Research B 286 (2012) 200–208

Contents lists available at SciVerse ScienceDirect

Nuclear Instruments and Methods in Physics Research B

journal homepage: www.elsevier.com/locate/nimb

Electronic excitations and defect creation in wide-gap MgO and $Lu_3Al_5O_{12}$ crystals irradiated with swift heavy ions

A. Lushchik [a,*], T. Kärner [a], Ch. Lushchik [a], K. Schwartz [b], F. Savikhin [a], E. Shablonin [a], A. Shugai [a], E. Vasil'chenko [a]

[a] Institute of Physics, University of Tartu, Riia 142, 51014 Tartu, Estonia
[b] Gesellschaft für Schwerionenforschung (GSI), Planckstr. 1, 64291 Darmstadt, Germany

ARTICLE INFO

Article history:
Received 1 September 2011
Received in revised form 12 October 2011
Available online 23 November 2011

Keywords:
Radiation defects
Non-impact mechanisms
Luminescence
Metal oxides

ABSTRACT

A comparative study of radiation effects in two groups of single crystals with an energy gap of about 8 eV possessing drastically different lattice and electron energy structures – fcc MgO and $Lu_3Al_5O_{12}$ with 160 atoms per a unit cell – has been performed using crystal irradiation with vacuum ultraviolet radiation, electrons, fast fission neutrons and, in particular, ~2.2 GeV uranium ions. In MgO with the absence of self-trapping for valence holes, the localization of holes near impurity ions or bivacancies (both as-grown or induced by a plastic stress) has been detected. In LuAG, the peculiarities of the motion of hole polarons and excitons, the radius of which is smaller than the size of a unit cell, have been revealed and analysed. The irradiation of MgO and LuAG with swift heavy ions providing an extremely high density of electronic excitations causes also the nonimpact creation of long-lived Frenkel defects in an oxygen sublattice.

1. Introduction

The coloration of NaCl ionic crystals under X-rays was investigated by Roentgen and Joffe back at the beginning of the 20th century, while Rutherford and Khariton noted that α particles caused irreversible damage to ZnS luminescent screens. However, a systematic study of radiation defects was started only after the first fission reactor was started in Chicago in late 1942. It was found that construction materials exhibit drastic changes under intense radiation. From this time, the important problem facing solid-state physics is the increase in radiation resistance of materials and the use of radiation technologies for improving different material characteristics.

By now it has been experimentally proved and theoretically justified that radiation defects in solids can be formed due to the universal knock-out (impact) mechanism connected with elastic collisions of high-energy incident particles with the ions of a crystal, thus, causing the creation of separated vacancies (v) and interstitials (i). This rapid impact creation mechanism of v–i pairs of Frenkel defects (FDs) is especially essential for the materials, where the formation energy of a pair of FDs exceeds the energy gap, $E_{FD} > E_g$.

However, in a number of metal halides, $E_{FD} < E_g$ and even $E_{FD} < E_{ea}$ (E_{ea} – the formation energy of an anion exciton). At the beginning of the 1960s, the first creation spectra of F centres (an electron in the field of an anion vacancy, $v_a e$) and i_a anion interstitials (according to the EPR study, a dihalide molecule X_2^- located at an anion site, i.e., an H centre) were measured for these materials. It was shown, that FDs are efficiently created via nonimpact mechanisms connected with the excitation and ionisation of an electron subsystem. Hundreds of papers have been devoted to the detailed investigations of the excitonic (e^0) and electron–hole (e–h) mechanisms of FD creation (see, e.g., [1–5] and references therein). It is worth noting that, according to the creation spectrum of F–H pairs, $E_{FD} > E_g$ in NaCl at $T < 150$ K, while stable (long-lived) pairs of FDs can be formed even at liquid helium temperature (LHeT) due to the recombination of hot (nonrelaxed) conduction electrons with self-trapped holes [6]. The efficiency of such hot e–h recombination is high at 8 K if the energy of exciting photons reaches 13–14 eV or photons of ~33.4 eV form cation excitations. The efficient creation of stable FDs at the decay of cation excitons ($h\nu \sim 62$ eV) has been also detected in LiF crystals [7]. By generalizing the results for some metal halides, we initiated the investigation of the role of hot recombination in the FD creation in metal oxides as well [8].

The experimentally determined threshold energy for a rapid impact mechanism of FD creation in many wide gap metal oxides (MgO, CaO, $MgAl_2O_4$, Al_2O_3, Y_2O_3, $Y_3Al_5O_{12}$, etc.) is about 50–60 eV (see [9] and references therein). According to theoretical estimates, this value is about twice lower for nonimpact adiabatic (slow, $\tau \sim 10^{-10}$ s) mechanisms of defect creation, i.e., still

* Corresponding author. Tel.: +372 7374619; fax: +372 7383033.
E-mail addresses: luch@fi.tartu.ee, aleksandr.lushchik@ut.ee (A. Lushchik).

0168-583X/$ - see front matter © 2011 Elsevier B.V. All rights reserved.
doi:10.1016/j.nimb.2011.11.016

exceeding the value of E_g. In MgO crystals with NaCl-type crystal lattice, an adiabatic decay of electronic excitations (EEs) into stable FDs in a regular region of a crystal lattice is additionally hampered by an especially high mobility of conduction electrons, valence holes and large-radius excitons. Neither e and h nor e^0 undergo self-trapping in a regular lattice of MgO (see, e.g., [10–13]).

In the present study, the role of EEs in the creation of v–i pairs of stable FDs is investigated on the example of MgO and $Lu_3Al_5O_{12}$ (LuAG) single crystals with $E_{FD} > E_g$ but with drastically different lattice and electron energy structure. In MgO, particular emphasis is laid on the influence of divalent and trivalent metal impurity ions on the efficiency of hot e–h recombination. Be^{2+} and Ca^{2+} impurity ions serve as low-temperature hole traps, while $[hBe]^+$ and $[hCa]^+$ Coulomb trapped-hole centres have a large cross-section for the recombination with conduction electrons (both cold and hot ones). The trapping of electrons occurs at Cr^{3+}, Fe^{3+}, etc., impurity ions or at bivacancies ($v_a v_c$), the number of which can be significantly increased, in particular, by an exposed plastic stress. An extremely high density of EEs, that is favourable for hot e–h recombination, was reached by the irradiation either with powerful single electron pulses of nanosecond duration or with ~2 GeV swift heavy ions (SHIs). In the latter case more than 99% of the absorbed energy is spent on ionisation losses (formation of EEs) [14,15] and it is likely that the processes of radiation defect creation by fast neutrons or SHIs are rather different even in highly radiation-resistant MgO single crystals – both practically hydrogen-free samples and MgO crystals enriched with OH^- or hydrogen ions (see, e.g., [16,17]).

The second investigation object – LuAG single crystals have a complex crystal lattice with 160 atoms per unit cell and have already been used for several applications [18]. Isostructural yttrium garnet ($Y_3Al_5O_{12}$ – YAG) has been thoroughly studied (see, e.g., [19,20]). However, a comparison study of virgin and dense-irradiated (with SHIs or single electron pulses) LuAG crystals was still needed. According to the theoretical analysis of intrinsic and impurity (defect-related) EEs in two-cation oxides, the effective radius of oxygen polarons (l) does not exceed the size of a large unity cell ($l_0 > 10$ nm), $l < l_0$. Therefore, one might expect peculiarities in migration of EEs and the nonimpact process of radiation defect creation in such complex metal oxides, especially under conditions of high and superhigh density of EEs. The present study is the first investigation of such radiation effects in LuAG.

Complex wide gap ($E_g > 6$ eV) metal oxides find application in different technical areas. Electron and hole small-radius polarons in polycation oxides exhibit inhomogeneous broadening of their energy spectra within a large unity cell. This circumstance along with the existing data on semiconductors with a complex electron-energy structure should be taken into account considering the interesting radiation effects in complex metal oxides. In semiconductors, the creation of radiation defects with the participation of EEs was suggested long ago to be the additional channel to the dominant impact mechanism [21].

2. Experimental

The experiments have been performed with single crystals of MgO and $Lu_3Al_5O_{12}$, virgin or preliminarily irradiated by vacuum ultraviolet (VUV) radiation, electrons, fast neutrons, X-rays and SHIs (U and Au). Nominally pure LuAG were grown by the Czochralski method under the atmosphere containing hydrogen from 5 N starting material in CRYTUP, Turnov, Czech Republic. MgO, MgO:Al^{3+}, MgO:Cr^{3+}, MgO:Be^{2+}, MgO:Ca^{2+} and MgO:OH^- single crystals were grown in Tartu from a highly pure starting material by a variation of the arc-fusion method.

The crystals were irradiated by SHIs at room temperature (RT) perpendicular to the (100) plane at the UNILAC linear accelerator of the GSI Darmstadt (see, e.g., [15]). The spectra of the induced optical absorption were measured in the spectral region of 6.5–1.5 eV using a double-beam spectrometer JASCO V-550 and in the region of 4.5–7.6 eV using a vacuum monochromator VMR-2. The thermally stimulated luminescence (TSL, 300–875 K) was measured at the heating of the previously irradiated samples with a constant rate of $\beta = 2$ K s^{-1} in the atmosphere of flowing nitrogen, using an Harshow Model 3500 TLD Reader or System 310 TLD Reader. It was possible to register a spectrally integrated (1.9–4.1 eV) signal or the TSL selected by optical filters. The spectra of steady cathodoluminescence (CL) were measured in the region of 1.6–11 eV (through double monochromators) at the excitation by an electron gun (5–15 keV, typically 300 nA and 2-mm^{-2} spot) at 6–420 K. After the electron irradiation was stopped, it was possible to register the spectra of phosphorescence at 6 K and the TSL curves at 6–420 K (for an integral signal or a certain emission selected through a double monochromator) of the irradiated sample with a constant heating rate of $\beta = 10$ K min^{-1}. The spectra of fast emissions were measured using powerful single electron pulses from the Kovalt'chyk–Mesyats type generator (3 ns, the current density 1–180 A cm^{-2}, 300 keV). The main photoluminescence experiments were carried out at the SUPERLUMI station of HASYLAB at DESY, Hamburg (see [22] for details). The excitation and reflection spectra (the angle of incidence on the (001) crystal surface was 17.5°) were normalized to equal the quantum intensities of the synchrotron radiation (4–35 eV) falling onto the crystal.

3. Radiation effects in MgO single crystals

Hundreds of papers and many reviews and monographs have been devoted to the radiation phenomena in pure and doped MgO single crystals containing also as-grown anion and cation vacancies (v_a and v_c) and bivacancies ($v_a v_c$) (see, e.g., [23–25]). Sufficiently pure and structurally perfect (without hydrogen, OH^- and $v_a v_c$) MgO crystals exhibit high resistance against radiation. The manifestations of free excitons in the form of line spectra of absorption (reflection) [26] and luminescence [27] as well as of near-impurity-localized excitons (e.g., near Ca^{2+} [10]) with the coexistence of line and broadband spectra have long been revealed.

In contrast to alkali halides, the lowest energy state of excitons in MgO is a singlet state with $j = 1/2$, while a triplet state with $j = 3/2$ possesses a higher energy. Such an energy structure of excitons fits naturally into the widely accepted scheme that at low temperatures excitons and holes do not undergo transition into a self-trapped state in regular lattice regions of MgO. On the other hand, according to luminescent and electron paramagnetic resonance (EPR) studies, even isovalent Be^{2+} and Ca^{2+} impurity ions can serve as hole traps. These trapped-hole centres are stable up to 190 and 50 K in MgO:Be and MgO:Ca, respectively, and the recombination of conduction electrons with $[hBe]^+$ and $[hCa]^+$ centres cause at LHeT broadband emissions peaked at 6.2 or ~6.8 eV [13]. It is worth noting that Coulomb $[hBe]^+$ and $[hCa]^+$ trapped-hole centres have a large cross-section for the recombination not only with cold electrons, relaxed to the bottom of the conduction band, but with hot (nonrelaxed) conduction electrons as well. The energy released at such hot e–h recombination in NaCl is sufficient for the creation of long-lived pairs of FDs even at LHeT [6]. Unfortunately, we have not succeeded as yet to provide experimental proof for the creation of FDs via hot recombination with the participation of Be- or Ca-related trapped-hole centres at the irradiation of MgO by synchrotron radiation of 8–20 eV. This failure is connected with a low probability of hot recombination under conditions of relatively low intensity and fluences of synchrotron radiation and with the competitive processes due to the presence of OH^- and hydrogen traces in our MgO samples. The situation is

even more complicated at $h\nu \geqslant 22$ eV, when the efficiency of complex Auger processes is high and one exciting photon of such energy is able to form even two e–h pairs (the so-called process of EEs multiplication [28,29]) in MgO. However, the energy released at the recombination of either of these pairs is insufficient (less than E_{FD}) for the creation of a pair of FDs.

At the same time, the irradiation of MgO causes the transformation of already existing as-grown defects [29–31]. At our disposal were MgO single crystals prepared by additive coloration (thermochemical reduction – TCR), wherein a crystal is heated in magnesium vapour at a high temperature. Such MgO(TCR) crystals contain F and F^+ centres (two or one electron in the field of v_a). Fig. 1 shows the excitation spectra for the luminescence of F^+ (3.2 eV) and F centres (2.4 eV) as well as the reflection spectrum measured in a MgO(TCR) crystal at 8 K using synchrotron radiation of 14–35 eV. At high values of reflection and absorption constants ($\geqslant 10^6$ cm^{-1}), a majority of the mobile EEs formed at the excitation reaches a surface (a "dead layer") and decays nonradiatively there. However, at $h\nu > 22$ eV the reflection is decreased by a factor of 20 and the value of absorption coefficient is practically constant. The luminescence efficiency of F and F^+ centres sharply increases at 25–30 eV (see Fig. 1), where each exciting photon forms a hot conduction electron able to create a secondary e–h pair. Both formed e–h pairs (primary and secondary ones) are situated spatially close to each other but relatively far from the surface. This experiment confirms the presence of F and F^+ centres in the whole volume of a MgO(TCR) sample.

The emission spectra of a MgO(TCR) crystal have been measured under irradiation by 5 keV electrons at 9 K (the spectra were registered 3 and 30 min after the electron irradiation was started). Fig. 2 presents the decomposition of this CL into three components – emissions of F and F^+ centres and earlier unidentified intense band at 2.9 eV (see, e.g., [32]). According to our additional investigations, the 2.9 eV emission can be attributed to the recombination of mobile hot holes with the electrons localized at v_a or v_av_c, which survive in the sample after its thermochemical reduction and subsequent cooling down to RT. The conduction electrons formed at the first stage of CL measurements (after 3 min) undergo rapid localization at v_av_c forming the so-called P^- centres ($[ev_av_c]^-$, see [24]), while a subsequent recombination of holes with P^- centres results in the emission at 2.9 eV or the dissociation of v_av_c with a subsequent formation of the additional number of F or F^+ centres. The 2.9 eV emission undergoes saturation with irradiation time and the emission of F and F^+ centres becomes clearly visible in the CL spectra measured after a prolonged electron irradiation (see Fig. 2b).

The presence of v_av_c in MgO(TCR) is supported by the excitation spectrum for 2.9 eV emission in a plastically deformed MgO crystal [33]. The broadband emission is efficiently excited in a wide

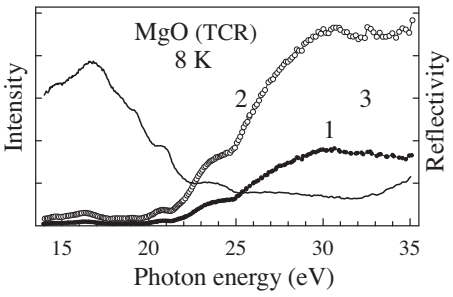

Fig. 1. Excitation spectra for the luminescence of F (2.4 eV, curve 1) and F^+ centres (3.2 eV, curve 2) as well as the reflection spectrum (3) measured in a thermochemically reduced MgO(TCR) crystal at 8 K using synchrotron radiation of 14–35 eV.

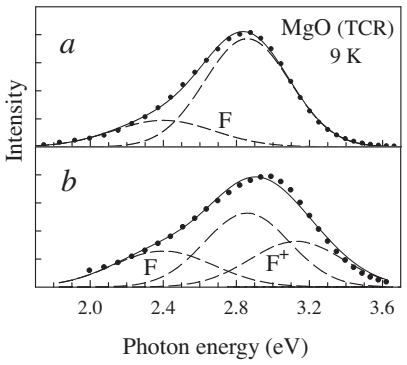

Fig. 2. Cathodoluminescence spectra (••) for a MgO(TCR) crystal measured in 3 (a) or 30 min (b) after irradiation by 5 keV electrons at 9 K was started. Components of decomposition (dashed lines) and their sum (solid line).

spectral region of 7.2–7.6 eV. Earlier such unusually wide excitation bands were detected in plastically deformed alkali halides and interpreted as the excitation of halogen ions situated at different sites with respect to a bivacancy [34]. The bivacancy-related excitation band in alkali halides extends from the region typical of the halogen excitation near a single v_a to exciton absorption (see [34] and references therein). The excitation bands connected with the intracentre excitation of the luminescence of F and F^+ centres in a MgO(TCR) crystal (this spectral region is not shown in Fig. 1) coincide with those reported earlier in the literature (see, e.g., [35]). To obtain crystals with single F and F^+ centres (without v_av_c), the growing of MgO single crystals by arc-fusion method should be performed very carefully – crystal growth as well as subsequent annealing and cooling must be done in an optimised atmosphere. It is the only way to avoid the formation of as-grown v_av_c and even more complex vacancy associations that are filled with hydrogen and cause light extinction (see, e.g., [35]). A total annealing of F^+, F-absorption occurs after the heating of MgO(TCR) up to ~1500 K thus providing a high mobility of not only interstitials but vacancies as well.

The irradiation of our MgO single crystals (annealed after crystallization and transparent up to 6 eV) by fast neutrons with an energy of 1–3 MeV and fluences up to 10^{17}–10^{18} n cm^{-2} induces optical absorption bands related to F^+ (4.96 eV, dominating in the spectrum), F (5.05 eV) and F_2 centres (3.48 eV) as well as the bands peaked at 2.3 eV, 2.1 eV and in a more long-wavelength spectral region. The presence of radiation-induced F, F^+ and F_2 bands is the supporting evidence for the creation of long-lived (stable) defects in an anion sublattice of MgO. On the other hand, the irradiation of MgO at RT does not practically cause the creation of cation FDs. According to the existing hypothesis [35], magnesium interstitials are mobile at RT, thus, facilitating the recombination within close pairs of cation FDs with the restoration of a regular lattice.

So far there is no strict experimental evidence supporting the suggestion [36] that the relatively high efficiency of F_2-centre creation by fast neutrons can be explained by a sequential formation of two F centres (in neighbour sites) and two oxygen interstitials by the same incident neutron. It is worth noting that the irradiation of MgO with SHIs (^{238}U, ~2 GeV, RT) leads to the efficient creation of F and F^+ centres, while a rather weak F_2-band is detected in the spectrum of radiation-induced optical absorption. The number ratio of F, F^+ and F_2 centres in an ion-irradiated MgO is significantly higher than that in a neutron-irradiated sample [37]. A further quantitative investigation of the reason of this difference lies ahead. Of particular interest is the creation of FDs at the end of ^{238}U range, where the impact mechanism of defect creation becomes a dominant one and causes even the peeling of an irradiated layer of a crystal in case

of sufficiently high ion fluences. The latter effect was revealed in LiF single crystals with a significantly lower resistance against radiation (as compared to MgO).

For the present, oxygen interstitials remain the least studied defects in metal oxides. Although the EPR detection of oxygen interstitials in MgO was reported already in [38], a further detailed investigation of anion interstitials has been performed recently in [39] and also in MgO crystals doped by Be^{2+} ions with an s^2 shell and a small ion radius. Using EPR and luminescence methods, it is shown that Be^{2+} serve as hole traps stable up to 190 K and, tentatively, as the traps for oxygen interstitials [40].

According to our long-standing experience, the impurity/defect-related recombination luminescence at $h\nu > 4$ eV in a crystal ($E_g \approx 8$ eV), previously irradiated by photons forming separated electrons and holes via band-to-band transitions, arises due to either the e–h recombination of conduction electrons with the holes localized near Ca^{2+} (emission at ~6.8 eV), Be^{2+} (~6.2 eV) or Al^{3+} impurity ions (emission at ~5.3 eV) or at the tunnel recombination between the electrons from shallow traps with localized holes. The mobile holes recombine with the electrons still localized at imperfections (h–e recombination) providing mainly emission in the spectral region of $h\nu < 4$ eV, i.e., below a half of E_g. So, the spectrum of recombination luminescence allows determining a sign of a mobile carrier in the related recombination process.

Basing on this empirical regularity we assumed that the important information on direct thermal ionisation of electron F centres created, for instance, by fast neutrons can be lost at the registration of high-temperature TSL using TLD Readers with a limited sensitivity region (1.9–4.1 eV). Fig. 3 shows the curves of TSL measured for a MgO:Al single crystal irradiated by fast fission neutrons (1–2 MeV, 10^{16} n cm^{-2}, RT). According to earlier EPR and luminescence investigations, our samples contain single Al^{3+} at Mg^{2+} sites as well as associations of Al^{3+} impurity ions with cation vacancies – $Al^{3+}v_c$, $Al^{3+}v_cAl^{3+}$ and a small amount of $Al^{3+}v_cOH^-$. The TSL curves were measured after a long storage of neutron-irradiated samples at RT in a wide temperature region of 300–870 K, while a thermal background was subtracted at $T > 620$ K. After repeated sequential heating RT → 870 K with $\beta = 2$ K s^{-1} resulting in a total bleaching of stored lightsum at $T < 750$ K, the sample was additionally weakly irradiated by X-rays (40 kV, 10 s, RT). The TSL measured for this sample using an optical filter (transparency region of 2.8–4.1 eV) consists of the peaks at 375 and 423 K, significantly weaker peaks at 565 and 625 K, and is totally absent at 700–870 K (see Fig. 3a).

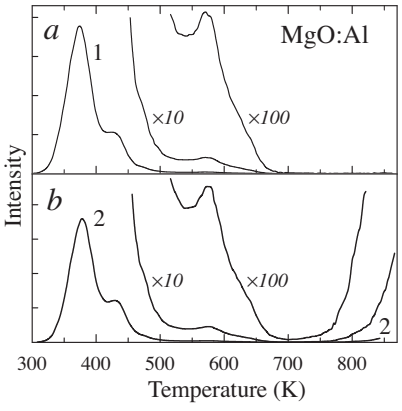

Fig. 3. TSL curves (1 and 2) measured for a MgO:Al single crystal irradiated by fast neutrons (1–2 MeV, 10^{16} n cm^{-2}, RT) and additionally just before measurements, weakly irradiated by X-rays (40 kV, 10 s, RT). TSL were registered through an optical filter (2.8–4.1 eV, part (a)) or the same filter and a glass spectral transformer (part (b), see text for details). For certain regions, the curves multiplied by a factor of 10 or 100 are shown as well. $\beta = 2$ K s^{-1}.

The same procedure was repeated for another identical neutron-irradiated MgO:Al sample but, in addition to an optical filter, a special glass transforming ultraviolet emission of 5–6 eV into orange light suitable for TLD Reader was used at the registration of the second TSL curve (see Fig. 3b). In such a manner, the 840 K peak was detected, so far as we know for the first time, in the TSL of ~5.3 eV typical of aluminium-related centres. The activation energy of this peak equals 2.2 eV and a frequency factor is about 10^{11} s^{-1}. In MgO irradiated with fast neutrons (10^{17} n cm^{-2}, RT), the TSL peak at ~740 K with $p_0 = 10^{11}$ s^{-1} has been detected as well [39].

It is important to compare the processes of FD creation by fast neutrons and ~2 GeV SHIs that transfer more than 99% of their energy to an electron sublattice. So far such comparison has been performed in details for LiF crystals in many laboratories. The investigation of the influence of SHIs on the same MgO crystals studied earlier under neutron-irradiation has been started as well. In particular, the creation of oxygen interstitials localized near the holes trapped by v_c was detected in neutron-irradiated MgO:Be crystals by means of EPR and optical methods [29,34–36].

Fig. 4a presents the TSL curves measured at 300–810 K for two MgO:Be single crystals irradiated with 2.5 GeV ^{238}U ions (10^{12} ions cm^{-2}, RT). Before ion-irradiation one of these identical samples was additionally exposed to plastic stress (~4%). In the sample exposed to a plastic stress there is a significant enhancement of the TSL peaks at 350–480 K measured through an optical filter, the transparency region of which (2.8–4.1 eV) covers the emissions of F^+ centres and oxygen ions nearby v_av_c. According to EPR investigations (see, e.g., [13]), these peaks are related to the release of holes from the centres that also contain v_c (peak at 420 K) or v_c and OH^- ions (peak at 360 K). Fig. 4b presents the TSL of the same two MgO:Be samples measured through an optical filter and a special glass that additionally transforms the Be-related emission at ~6.2 eV into an orange light. Although the 6.2 emission at high temperatures is relatively weak, there is a clear increase in the intensity of the TSL at 760–810 K in the sample exposed to the plastic stress and subsequent irradiation with SHIs.

The irradiation with SHIs induces the deformation of a crystal, leads to the disordering of a regular lattice and accelerates ionic diffusion along weakened (reduced-symmetry) lattice sites. So, the appearance of the TSL peak at ~800 K in the stressed MgO:Be can be tentatively ascribed to the diffusion of interstitials along reduced-symmetry sites of a deformed lattice.

It should be pointed out that the efficiency of nonimpact creation of radiation defects in highly pure MgO is low. Hence, it is

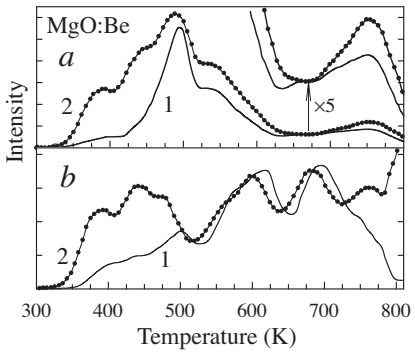

Fig. 4. TSL curves (1, 2) measured for two MgO:Be single crystals irradiated with 2.5 GeV ^{238}U ions (10^{12} ions cm^{-2}, RT). Before ion-irradiation one sample (curves 2) was additionally exposed to plastic stress (~4%, RT). The TSL were registered through an optical filter (2.8–4.1 eV, part (a)) or the same filter and a glass spectral transformer (b). $\beta = 2$ K s^{-1}.

promising to use highly sensitive luminescent methods instead of a conventional method of optical absorption.

Turning back to the contribution of hot e–h recombination to the creation of stable FDs in MgO, it should be pointed out that favourable conditions for the realization of this mechanism appear at the decay of cation excitons formed by 52–58 eV photons. The manifestations of these cation excitons have long been detected in the reflection spectra of single crystals and the absorption spectra of thin films. Deep dips in the creation region of cation excitons have been revealed in the excitation spectrum of Al^{3+}-related broadband emission at ~5.3 eV in a MgO:Al single crystal [28]. The 5.3 eV emission efficiency in the region of these dips (52–58 eV) is approximately the same as at $h\nu \approx 32$ eV. The energy loss (20–25 eV > E_{FD}) is basically sufficient for a slow (~10^{-10} s) adiabatic creation process of a stable FD pair. Unfortunately, direct experimental proof of the decay of cation excitons into stable FDs in MgO is yet to be proved. In contrast to a similar task for NaCl with cation excitons at 33–36 eV [6], the spectral region of 50–70 eV is rather inconvenient for synchrotron experiments. Cation excitons are considered as localized EEs. The hopping diffusion of self-trapped excitons and self trapped holes in alkali halides has been considered in [41].

4. Radiation effects in lutetium garnet

Similar to YAG, thoroughly studied during the past decade, isostructural LuAG crystals are very promising for application due to their high macrosymmetry, density (~6.7 g cm^{-3}) and assumed high radiation resistance (at least against X- and γ-rays). However, the interpretation of physical processes in polycation oxides is rather difficult because of the complex microstructure of garnets. Furthermore, LuAG contains a rare-earth Lu^{3+} cation with a fulfilled $4f^{14}$ inner shell and complex electron energy structure. By now the latter has been precisely interpreted only for LuF_3, $LiLuF_4$ and $LiYF_4$:Lu^{3+} [42]. In LuAG, Lu^{3+} possess a wide variety of discrete $4f^{14} \leftrightarrow 4f^{14}$ transitions, while interconfiguration $f^{14} \leftrightarrow f^{13}d^1$ electron transitions are expected slightly below 11 eV (such transitions are detected at about 11 eV in fluorides).

A comparative investigation of reflection and absorption spectra, as well as different luminescent characteristics has been performed for LuAG single crystals – virgin or previously irradiated with 2.14 GeV ^{238}U ions (fluence of 10^{12} ions/cm^2) at RT. Fig. 5 presents the reflection spectra measured for virgin and U-irradiated LuAG single crystals using synchrotron radiation of 5–19 eV at 10 K. The irradiation with SHIs causes the increase of the reflection constant in the spectral region of 7–18.6 eV. The ratio of the reflection spectra for the irradiated and virgin samples R_{irr}/R_{vir} is shown in the respective figure as well. The value of R_{irr}/R_{vir} at $h\nu$ = 15–16 eV is about three times as high as at 6–7 eV. It is necessary to stress that one of the main reflection maxima in α-Al_2O_3 is located at 16 eV (LHeT). An especially sharp rise of R_{irr}/R_{vir} occurs at 11–12 eV that is close to the region where $f^{14} \leftrightarrow f^{13}d^1$ interconfiguration electron transitions in Lu^{3+} are expected. It seems plausible that in this spectral region we see the manifestation of a ionisation of Lu caused by SHIs.

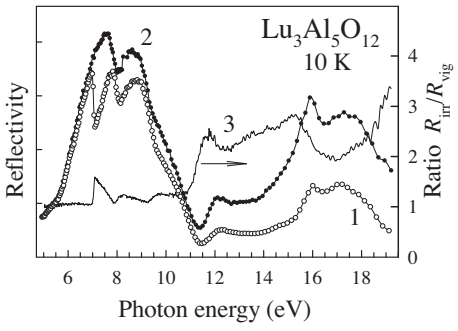

Fig. 5. Reflection spectra measured for a virgin LuAG single crystal (curve 1) and the sample previously irradiated with ^{238}U ions (2.14 GeV, 10^{12} ions cm^{-2}, RT, curve 2) using synchrotron radiation at 10 K. The ratio of the reflection spectra for irradiated and virgin samples (curve 3).

Fig. 6 shows the optical absorption spectra measured at RT for virgin and uranium-ion-irradiated LuAG crystals at RT. The range of ^{238}U ions was about 50 μm. The radiation-induced absorption (difference between the spectra after and before irradiation) is especially high at 6.0–6.6 eV and at $h\nu$ > 7.5 eV. This difference spectrum consists of well-known bands related to F and F^+ centres (peaked at 6.05 and 5.4, 3.5 eV, respectively [18,43–45]). So, the sample kept after ion-irradiation for a month in darkness and without any contact with an atmosphere still contains a certain amount of radiation-created F and F^+ centres. The last conclusion is clearly supported by the excitation spectra measured at 10 K for the 2.8 eV emission of F centres and 3.15 eV emission of F^+ centres in the LuAG previously irradiated with ^{238}U ions (see Fig. 6). The figure also presents the excitation spectrum for a broadband emission peaked at ~4.5 eV, which is conclusively interpreted in the literature as the emission of antisite defects $Lu|_{Al}$ – Lu^{3+} ion at Al^{3+} site [18,43]. The concentration of such as-grown antisite defects is significantly lower in a thin crystalline film of LuAG, prepared by liquid phase epitaxy technology at about 1000 °C, i.e., significantly below the melting temperature (~2000 °C) [46]. The analysis of the data presented in Figs. 5 and 6 allows us to conclude that the additional numbers of F, F^+ and $Lu|_{Al}$ centres are created by the irradiation of LuAG with SHIs, more than 99% energy of which is transferred to an electron subsystem of a crystal.

In YAG, the low-temperature emission at 4.9 eV is convincingly attributed to the radiative decay of mobile anion excitons [20,43,47]. However, these excitons differ strongly from the free excitons with line absorption and emission spectra in MgO as well as from "self-shrunk" excitons in α-Al_2O_3, which give a broadband emission (~7.6 eV) at the excitation by 9.1 eV photons [48]. In α-Al_2O_3, the quantum yield of photoconductivity in the region of exciton absorption is by several orders of magnitude lower than in the region of band-to-band transitions, $h\nu$ > 9.6 eV (see [48] and references therein).

Besides the emission of antisites at 4.5 eV, a broad emission band at 4.9–5.1 eV has been detected already during the first measurements of cathodo- and photoluminescence of LuAG at LHeT. Some authors tentatively interpret this broad emission as the intrinsic exciton luminescence (our present experimental data

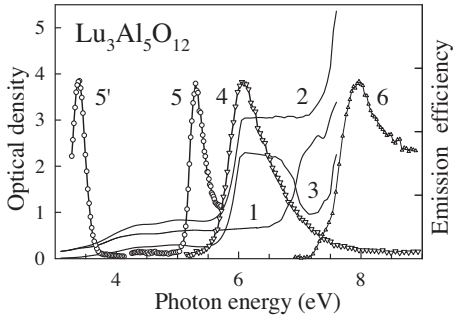

Fig. 6. Optical absorption spectra measured at RT for virgin (curve 1) and uranium-ion-irradiated (2.14 GeV, 10^{12} ions cm^{-2}, RT, curve 2) LuAG crystals at RT. The difference between the absorption spectra after and before irradiation (3). The excitation spectra measured at 10 K for the 2.8 eV emission of F centres (4), 3.15 eV emission of F^+ centres (curves 5 and 5′) and 4.5 eV emission (curve 6) of $Lu|_{Al}$ antisite defects in LuAG previously irradiated with ^{238}U ions.

support this point of view as well), while others attribute it to another type of antisite defects.

Fig. 7a shows the temperature dependences of the intensity of 4.50 ± 0.15 and 5.2 ± 0.25 eV emissions selected though a double monochromator at the steady excitation of a LuAG crystal by 5-keV electrons (300 nA mm^{-2}). The dependence was measured at the crystal cooling with a constant rate of $\beta = 10$ K min^{-1} under the level of vacuum of about 10^{-7} torr. The intensity of the 4.5 eV emission slightly varies at 275–135 K ($\leqslant$20%) and decreases by a factor of 2 from 130 to 6 K. On the other hand, a step-by-step increase in the 5.2 eV emission intensity occurs at the crystal cooling 300 → 40 K (plateaus at 220–180 and 90–70 K). The peculiarities of the 5.2 emission behaviour below 40 K are partly caused by the changes in the cooling rate under steady electron beam irradiation. It is worth noting that 1 s after the electron irradiation at 6 K was stopped, the intensity of the 5.2 eV emission decreased by at least 4 orders of magnitude (down to the noise level), while the more intense 4.5 eV emission weakens in a second by 3 orders of magnitude and continues its damping by a factor of 10 in a few minutes. Thereafter prolonged tunnel phosphorescence was detected in a wide spectral region of 1.8 eV (apparatus limit) to about 4 eV.

Fig. 7a also presents the TSL curves measured for a LuAG crystal previously irradiated by 5-keV electrons at 6 K. The curves are registered for a spectrally integrated signal (1.8–6.0 eV) or for the 5.0 ± 0.3 eV emission selected through a monochromator (the latter signal is multiplied by a factor of 30). The ~200 K peak of integral TSL mainly consists of the recombination luminescence of Ce^{3+} impurity ions, a small amount of which (1–2 ppm) is present in nominally pure LuAG. The emission of 5 eV is practically absent in TSL above the main peak at 87 K and a weak one at 115 K.

The thermal stability of the EPR signal of the assumed self-trapped holes (in a form of O^- ions) was investigated in a LuAG single crystal doped with Sc^{3+} ions [18]. Pulse annealing of the EPR signal occurs between 75 and 140 K. However, according to [43], this EPR signal was not found in nominally pure LuAG crystals without scandium impurity ions (including the objects of the present study).

We have studied the kinetics of luminescence bands in the region of 1.9–6.0 eV at the excitation of LuAG crystals by single electron pulses at 80–300 K (3 ns, 300 keV, 80 A cm^{-2}, 30 s pause between two sequential pulses). Of particular interest were broadband emissions peaked at 4.5 eV ($Lu|_{Al}$ antisite defects) and ~5 eV in virgin LuAG crystals. Similar to the 4.9 eV emission in YAG [20,47], the 5 eV luminescence in LuAG can be tentatively ascribed to unusual excitons with the radius smaller than the size of a unit cell containing 160 atoms (8 molecules of $Lu_3Al_5O_{12}$). The detailed analysis of the kinetics data will be presented in a separate paper. Below only some results on this topic will be presented.

Fig. 8 demonstrates the emission spectra (pulse amplitude A was registered) measured at 80 K for virgin and ion-irradiated LuAG crystals. Besides Ce^{3+} luminescence (2.4 eV), the emissions with the maxima at 4.9 ± 0.2 eV and 4.5 ± 0.2 eV are clearly distinguished in the spectrum for a virgin LuAG. Any emission kinetics can be described by two exponents (further on these components will be reported as "short" and "long"). The decay times for ~5 eV emission at 80 K equal 0.5 and 1.6 μs, while a crystal heating to RT causes the shortening of a short component down to 9 ns. Fig. 7b presents the temperature dependence of the 5 eV emission at the excitation of LuAG by single nanosecond electron pulses. In contrast to the inertial recombination TSL of 5 eV that is practically vanished above 130 K (see Fig. 7a), the integral ($A \times \tau[T]/\tau[80\ K]$) of a long component of the 5 eV emission remains constant till ~160 K and starts to decrease above this temperature. The integral of a short component decreases at $T > 225$ K. The decrease of a pulse amplitude for the long 5 eV emission occurs above 240 K,

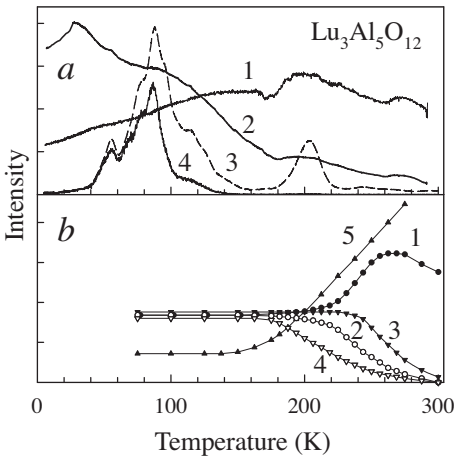

Fig. 7. (a) Temperature dependences of the intensity of 4.5 eV (curve 1) and 5.2 eV emission (curve 2) at the steady excitation of a LuAG crystal by 5-keV electrons (300 nA mm^{-2}). TSL curves measured ($\beta = 10$ K min^{-1}) for a spectrally integrated signal (1.8–6.0 eV, curve 3) or for the 5.0 eV emission (4) in a LuAG crystal previously irradiated by 5-keV electrons at 6 K. (b) Temperature dependence of short (1, 2) and long (3, 4) components of the 5 eV emission as well as of Ce^{3+} emission (2.4 eV, curve 5) at the excitation of LuAG by single nanosecond electron pulses. The emission pulse amplitude (1, 3, 5) or emission integral (2, 4) were registered. See the text for details.

while the value of A for a short component increases at 220–260 K and only then decreases at $T > 275$ K. According to Fig. 7b, the efficiency of 2.4 eV emission (about 3 ppm of Ce^{3+} ions in our LuAG sample) is low at the electron-pulse excitation at 80–140 K ($\tau \sim$ 50–60 ns) and A starts to increase in the temperature region where the 5.0 eV TSL is quenched, in parallel with the rise of τ up to 100–130 ns.

The analysis of the experimental data presented in Figs. 7 and 8 agrees with the attribution (see [18] and more solid evidences related to ~4.9 eV emission in YAG [20,47]) of the ~5 eV emission in LuAG to unusual excitons of small radius as compared to the size of a unit cell. The specific character of the motion of such excitons is determined by the possible hopping diffusion of small-radius hole polarons inside a complex oxygen sublattice. The values of activation energy and frequency factor have been determined for TSL peaks at 80–150 K in LuAG:Ce^{3+} [43]. However, in our opinion, the obtained enormously low values of $p_0 = 10^9$–10^{11} s^{-1} can not be explained only by a large number of hops of a hole polaron needed to reach a luminescence centre, and probably are connected also with the frequency of a hoping diffusion of "heavy" small-radius polarons ($l < l_0$).

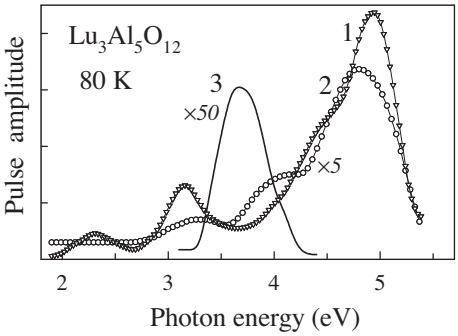

Fig. 8. Emission spectra (pulse amplitude A was registered) measured at 80 K for a virgin (1) or an ion-irradiated LuAG crystal (2.14 GeV, 10^{12} ions cm^{-2}, RT, curve 2). The enhancement of emission peak amplitude in an ion-irradiated crystal (3).

According to Fig. 8, the irradiation of LuAG with SHIs weakens the emission at 4.3–5.3 eV by a factor of 5. The emission was collected from the irradiated crystal surface and its weakening is partly caused by a substantial reabsorption in 50-μm irradiated layer, while the range on incident 250-keV electrons was about 150 μm. The enhancement of the emission peak amplitude is detected only at 3.25–4.25 eV. There are two maxima of this enhanced emission (curve 3 in Fig. 8) – the main component at ~3.75 and a weak one at ~4.05 eV. The fast 3.75 eV emission tentatively arises at the end of ^{238}U ion range (~50 μm), where ions come to a stop and cause an essential crystal stress. The absolute enhancement of the emission at ~3.75 eV was detected due to its short decay time (~70 ns) at 80 K. The emission undergoes thermal quenching already at 125 K. If the opposite, unirradiated surface of LuAG is excited by electron pulses, there is no ~3.75 eV emission at all. The TSL peaks at 90 and 115 K (see Fig. 9) measured for the ~3.7 eV emission (i.e., <0.5 E_g) tentatively correspond to the release of a hole from a trap and its movement towards an electron trapped by an ion-irradiation-induced defect, likely $v_a v_c$.

The creation spectra of some TSL peaks by VUV radiation have been measured for the purpose of separating the contribution of oxygen and lutetium (cation) excitons or separated electrons and holes to the transformation of pre-irradiation (as-grown) defects and the creation of novel radiation FDs in LuAG crystals. The crystal was irradiated by an equal quantum dose of VUV radiation (~10^{13} photons cm^{-2}) from a hydrogen discharge source at each of several energies (7.5–11.5 eV) at 80 K. The reference signal for normalization was recorded from a sodium salicylate. TSL was measured with β = 10 K min^{-1} and the light sum (or peak intensity) of a TSL peak was taken as a measure of the centres created by VUV radiation and responsible for this peak.

Fig. 9 shows the creation spectra of the TSL peaks at 90 and 115 K connected with hole centres and measured using the above-mentioned procedure in LuAG. The figure also presents the reflection spectrum measured for the same sample using synchrotron radiation of 7–13 eV at 80 K. The creation efficiency of the TSL peaks starts to rise at 7.5 eV testifying to the beginning of a weak ionisation. Similar to YAG [20], the rise of the ionisation efficiency at 7.6–8.0 eV reproduces the Urbach tail of exciton absorption in LuAG at 80 K.

The spectra of two-photon absorption (TPA) can provide important information on intrinsic EEs in strictly oriented LuAG single crystals. Unfortunately, at present there exist only the TPA spectra measured in our laboratory in Tartu at 80 or 300 K for high-quality YAG crystals grown by the method of oriented crystallization in Saint-Petersburg, Russia. It was mentioned already that YAG and LuAG are isostructural materials. A comparison of the spectra of one and two-photon absorption was performed for YAG [47]. At

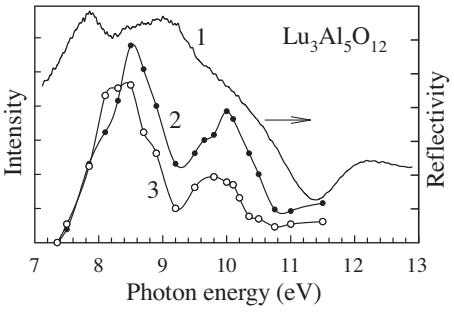

Fig. 9. Reflection spectrum (curve 1) measured for a LuAG crystal using synchrotron radiation at 80 K. The creation spectra of the TSL peaks at 115 K (curve 2) and 90 K (3) measured for LuAG after isodose (10^{13} photons cm^{-2}) VUV irradiation at 80 K (see the text for details).

80 K, two narrow peaks at 7.2 and 9.0 eV have been detected in the spectrum of TPA. The second peak is situated in the region of exciton absorption band in α-Al_2O_3, where aluminium ions occupy octahedral interstitial sites in the closely packed oxygen lattice. At the same time, the first peak of TPA is found at a significantly higher energy than the exciton absorption band in Y_2O_3. In a unit cell of YAG 16 Al^{3+} ions are located at octahedral sites (C_{3i} symmetry) while the other 24 aluminium ions are within oxygen tetrahedrons. Just tetrahedral aluminium–oxygen clusters are tentatively responsible for a long-wavelength region of the TPA spectrum in YAG. Isostructural LuAG crystals exhibit very close spectral characteristics.

Returning to the creation spectra of TSL peaks in LuAG presented in Fig. 9, we can note that the creation efficiency of the TSL peaks at 90 and 115 K is low in the regions related to the excitation (not ionisation) of tetrahedral aluminium complexes (7.4–7.5 eV) as well as of the octahedral ones (~9.2 eV). The third region (10.5–11.5 eV) where recombination luminescence (TSL) is weakly excited coincides with the region of efficient $f^{14} \leftrightarrow f^{13}d^1$ electron transitions in Lu^{3+} (these transitions have been recently investigated in metal fluorides [42]). The irradiation of LuAG with the photons that form lutetium cation exitons (10.5–11.5 eV) does not lead to the efficient excitation of recombination TSL. On the other hand, intense TSL was detected after the irradiation of LuAG with synchrotron radiation of a higher energy.

5. Concluding remarks

In metal oxides, peculiarities of the behaviour of hole polarons have been discussed over a long time [47,49–52]. A comparative study of several radiation phenomena has been conducted in wide gap ($E_g \approx 8$ eV) MgO and LuAG single crystals with very different crystal and electron energy structures under excitation with VUV radiation, electrons, fast neutrons and SHIs. The study continues the analysis of the peculiarities of radiation effects in different wide gap inorganic dielectrics (see, e.g., the Proceedings of some conferences [53,54]).

In regular regions of an MgO crystal with a high symmetry, the irradiation providing a low density of EEs leads to the formation of highly mobile free large-radius excitons as well as of electrons and holes which do not undergo self-trapping. Pairs of stable FDs are not created at the e–h recombination ($E_{FD} > E_g$), while efficient defect creation occurs under MgO irradiation by fast neutrons via the universal knock-out (impact) mechanism. In doped MgO crystals, holes are localized near Be^{2+} and Ca^{2+} ions substituting Mg^{2+} cations. Such Coulomb trapped-hole centers are stable up to 190 K ($[hBe]^+$) or 50 K ($[hCa]^+$) and possess a large cross-section for the recombination with cold or hot conduction electrons. However, these recombinations do not lead to the creation of stable FDs if the energy of a hot electron is sufficient for the beginning of the EEs multiplication process when the energy excess of a hot electron (with respect to the bottom of a conduction band) is used for the formation of a secondary exciton or a secondary e–h pair (see, e.g., [48,55]). These elementary mechanisms of EEs multiplication are in competition with the creation of FDs via hot e–h recombination. In MgO, the number of secondary e–h pairs is significantly higher than that of secondary excitons. Under conditions of low excitation density of MgO, both primary and secondary e^0 with a large radius and low oscillator strength interact mainly with impurity ions or lattice defects causing the appearance of their luminescence (e.g., of Cr^{3+}, Ge^{2+}, Mn^{2+} ions) or photodissociation (e.g., about 3.8 eV is needed for the dissociation of OH^-).

The situation is significantly more complicated in case of high density of radiation-induced EEs. The coexistence of free and self-trapped excitons (FEs and STEs), the energy states of which

are separated by an activation barrier, was experimentally revealed in alkali iodides long ago (see [3,4] and references therein). The presence of the activation barrier allows registering the emission of FEs at LHeT. The emission of weakly bounded biexcitons slightly shifted toward low energies as compared with FE emission was detected at high-dense excitation of KI and RbI as well (see, e.g., [56–58]). It was shown that the increase of the excitation density at low temperatures causes both the typical emission of biexcitons and the formation of F-H pairs of FDs. In KI and RbI at 5 K, $E_{FD} > E_g$ but $E_{FD} < 2E_{ea} \approx 12$ eV. So, the creation of FDs is possible at the decay of biexcitons. Even more favorable conditions for FDs creation arise at the interaction of a FE with a STE (a long-lived one!).

Only short-lived and highly mobile large-radius excitons exist in the bulk of MgO single crystals. The emission of biexcitons in MgO has not been yet detected. It is worth noting that even though the formation of biexcitons at a high-dense excitation is possible, the energy released at the nonradiative decay of a biexciton (about 16 eV) is insufficient for the creation of a pair of FDs in the bulk of a perfect MgO single crystal consisting of two-valent ions. On the other hand, intrinsic radiation defects can be also created via some nonimpact mechanisms at the irradiation of MgO with SHIs providing an extremely high density of EEs in ion tracks. This conclusion is based on the detailed comparison of the spectra of luminescence and radiation-induced absorption as well as of their thermal annealing in MgO crystals preliminarily irradiated with fast fission neutrons or SHIs (see also [59]). It is commonly accepted that F, F^+ and F_2 centres are formed via a universal impact mechanism (elastic collisions) in case of neutron-irradiation, while the dominant part of the energy of 2–3 GeV SHIs is transferred to an electron subsystem. In our opinion, the formation of cation EEs with the energy of 52–65 eV, which correspond to localized and long-lived (in comparison with a period of lattice vibrations) 2p and 3s excited states of Mg^{2+} regular cations, can be, in principal, accompanied by the creation of stable FDs (see also [28,60]). Certainly, more complicated processes of defect creation should be also taken into account at the joint action of impact and nonimpact mechanisms (see [14,15,21,33] and references therein).

Isostructural to LuAG stoichiometric $Y_3Al_5O_{12}$ single crystals with high melting temperature (above 2200 K) possess a record high radiation resistance among other wide-gap oxides – the formation energy of oxygen FDs $E_{FD} > E_g \approx 8$ eV. The validity of the latter inequality is supported by a theoretical estimation [61] of the energy needed for the formation of spatially separated (non-interacting) an anion vacancy and interstitial oxygen. The calculated energy is about 10 eV and it is an underestimated value because the energy consumption on the initial separation of FDs was not taken into account.

The behavior of stoichiometric LuAG crystals under irradiation of different types is studied insufficiently. The creation of F^+, F centres and antisite defects has been detected by direct absorption or highly sensitive luminescent methods in LuAG irradiated with 2.14 GeV ^{238}U ions. According to theoretical calculations [61], the formation energy of antisite defects is lower as compared with a pair of stable oxygen FDs. In LuAG complex two-cation crystals with 160 atoms per unit cell, low-energy excitons are connected with the excitation and partial ionization of either tetrahedral and octahedral aluminium–oxygen clusters (~7.4 and ~9.2 eV, respectively) or the excitation of lutetium ions (cation excitons, 10.5–11.5 eV). The energy of both oxygen exciton types is insufficient for the creation (not transformation!) of FDs. A detailed study of a fine structure and the process of hopping diffusion of the first type excitons (tetrahedral clusters), the radius of which is smaller than the size of a unit cell and a low-temperature broadband emission lies in a short-wavelength region as compared to the emission of as-grown antisite defects $Lu|_{Al}$ (~5 and 4.5 eV, respectively), still lies ahead. It is hoped that the method of two-photon absorption will be especially useful for this study. Earlier the TPA measurements had a determining role in the interpretation of excitons in YAG [47].

According to our experimental data, the radiation resistance against SHIs (~2.1 GeV, ^{238}U) of nominally pure LuAG single crystals grown by the Czochralski method is significantly lower than that of MgO single crystals. MgO crystals sustain a fluence of $\Phi = 10^{13}$ U cm^{-2}, while the ion-irradiation at $\Phi = 10^{12}$ ions cm^{-2} was used for the investigation of LuAG crystals (cracking of the samples occurs already at $\Phi = 3 \times 10^{12}$ ions cm^{-2} ions). The irradiation of LuAG even with $\Phi = 10^{12}$ ions cm^{-2} ions provides a high density of EEs and causes a significant attenuation of exciton emission (5 eV) as well as the creation, in addition to the as-grown structural defects, of F, F^+ centers and still unidentified defects responsible for the broadband emission peaked at ~3.7 eV. The investigation of the contribution of cation excitons (~11 eV) and more high-energy EEs to the creation and transformation of structural defects in LuAG lies ahead.

In conclusion it should be mentioned that a number of wide gap (E_g = 8–10 eV) metal oxides can be arranged in order of macrosymmetry reduction and increasing the size and complexity of a unit cell as $MgO \rightarrow Al_2O_3 \rightarrow MgAl_2O_4 \rightarrow Y_3Al_5O_{12}$, $Lu_3Al_5O_{12}$. There are substantial changes in the optical characteristics and mobility of low-energy excitons and holes (in a form of O^-) in this sequence: line absorption and emission spectra of highly mobile (like in semiconductors) free excitons in MgO; self-shrunk excitons and the absence of hole self-trapping in α-Al_2O_3 [48]; and, finally, participating in hopping diffusion excitons, the radius of which is significantly smaller than the size of a unit cell, in YAG and LuAG. In YAG, these excitons were clearly separated from the near-defect-localized excitons by measuring the dependence of exciton luminescence on the power of laser excitation – there is no saturation for the emission of intrinsic excitons [62]. It should be pointed out that at the irradiation of complex polycation oxides, a slow hopping diffusion of "heavy" EEs impedes their movement to the surface and subsequent nonradiative decay into structural defects.

Acknowledgements

We are grateful to Dr. M. Nikl for LuAG samples and to Drs. A. Kotlov and V. Nagirnyi for assistance in synchrotron measurements. The research leading to these results has received funding from the European Community's Seventh Framework Programme (FP7/2007-2013) under Grant agreement No. 226716 and the Estonian Science Foundation (Grant No. 7825).

References

[1] N. Itoh, A.M. Stoneham, Material Modification by Electronic Excitation, Univ. Press, Cambridge, 2000.
[2] Ch.B. Lushchik, I.K. Vitol, M.A. Elango, Usp. Fiz. Nauk 122 (1977) 223 (Sov. Phys. Usp., 20 (1977) 489).
[3] Ch.B. Lushchik, in: R.A. Johnson, A.N. Orlov (Eds.), Physics of Radiation Effects in Crystals, North-Holland, Amsterdam, 1986 (Chapter 8).
[4] Ch.B. Lushchik, A.C. Lushchik, Decay of Electronic Excitations with Defect Formation in Solids, Nauka, Moscow, 1989.
[5] K.S. Song, R.T. Williams, Self-Trapped Excitons, second ed., Springer, Berlin, 1996.
[6] E. Feldbach, A. Lushchik, Ch. Lushchik, V. Nagirnyi, E. Shablonin, S. Vielhauer, in: U. Johansson, K. Lilja, A. Nyberg, R. Nyholm (Eds.), MAX-LAB Activity Report 2010, Lund, Sweden, 2010, p. 462.
[7] S. Nakonechnyi, T. Kärner, A. Lushchik, Ch. Lushchik, V. Babin, E. Feldbach, I. Kudryavtseva, P. Liblik, L. Pung, E. Vasil'chenko, J. Phys: Condens. Matter 18 (2006) 379.
[8] A. Lushchik, Ch. Lushchik, M. Kirm, V. Nagirnyi, F. Savikhin, E. Vasil'chenko, Nucl. Instrum. Methods B 250 (2006) 330.
[9] A.I. Popov, E.A. Kotomin, J. Majer, Nucl. Instrum. Methods B 268 (2010) 3084.
[10] E.Kh. Feldbach, Ch.B. Lushchik, I.L. Kuusmann, Zh. Eksp. Teor. Fiz. Pis'ma Red. 39 (1984) 54 (JETP Lett. 39 (1984) 61).
[11] Ch. Lushchik, I. Kuusmann, V. Plekhanov, J. Lumin. 18/19 (1979) 11.
[12] P.V. Sushko, A.L. Shluger, C.R. Catlow, Surf. Sci. 450 (2000) 153.

[13] S. Dolgov, T. Kärner, A. Lushchik, A. Maaroos, S. Nakonechnyi, E. Shablonin, Fiz. Tverd. Tela 53 (2011) 1179 (Phys. Solid State 53 (2011) 1244).
[14] M. Toulemonde, S. Bouffard, F. Studer, Nucl. Instrum. Methods B 91 (1994) 108.
[15] K. Schwartz, G. Wirth, C. Trautmann, T. Steckenreiter, Phys. Rev. B 56 (1997) 10711.
[16] Y. Chen, M. Abraham, L.C. Templeton, W.P. Unruh, Phys. Rev B 11 (1975) 881.
[17] R. Gonzales, I. Vergara, D. Caceras, Y. Chen, Phys. Rev. B 65 (2002) 224108.
[18] M. Nikl, V.V. Laguta, A. Vedda, Phys. Status Solidi B 245 (2008) 1701.
[19] Yu.K. Voron'ko, B.I. Denker, V.V. Osiko, A.M. Prokhorov, M.I. Timoshechkin, Dok. Akad. Nauk SSSR 188 (1969) 1258 (Sov. Phys. Dokl. 14 (1970) 998).
[20] A.I. Kuznetsov, V.N. Abramov, V.V. Mürk, B.R. Namozov, Trudy Inst. Fiz. Akad. Nauk EstSSR 63 (1989) 19.
[21] N. Itoh, D.M. Duffy, S. Khakshouri, A.M. Stoneham, J. Phys.: Condens. Matter 21 (2009) 474205.
[22] G. Zimmerer, Radiat. Meas. 42 (2007) 859.
[23] B. Henderson, E. Wertz, Adv. Phys. 17 (1968) 749.
[24] B. Henderson, E. Wertz, Defects in the Alkaline Earth Oxides, Taylor & Francis, London, 1977.
[25] Ch. Lushchik, A. Lushchik, T. Kärner, M. Kirm, S. Dolgov, Izv. VUZ. Fiz. 43 (N3) (2000) 5 (Russ. Phys. J. (USA), 43 (2000) 171).
[26] C.R. Whited, W.C. Walker, Phys. Rev. Lett. 22 (1969) 1428.
[27] Ya.V. Valbis, K.A. Kalder, I.L. Kuusmann, Ch.B. Lushchik, A.A. Ratas, Z.A. Rachko, M.E. Springis, V.M. Tiit, Zh. Eksp. Teor. Fiz. Pis'ma Red. 22 (1975) 83 (JETP Lett. 22 (1975) 36).
[28] A.N. Vasil'ev, V.N. Kolobanov, I.L. Kuusmann, Ch.B. Lushchik, V.V. Mikhailin, Sov. Phys. Solid State 27 (1985) 1616.
[29] M. Kirm, E. Feldbach, T. Kärner, A. Lushchik, Ch. Lushchik, A. Maaroos, V. Nagirnyi, I. Martinson, Nucl. Instrum. Methods B 141 (1998) 431.
[30] M.A. Monge, A.I. Popov, C. Ballesteros, R. Gonzales, Y. Chen, E.A. Kotomin, Phys. Rev. B 62 (2000) 9299.
[31] V.N. Kuzovkov, A.I. Popov, E.A. Kotomin, M.A. Monge, R. Gonzalez, Y. Chen, Phys. Rev. B 64 (2001) 064102.
[32] A. Lushchik, T. Kärner, Ch. Lushchik, E. Vasil'chenko, S. Dolgov, V. Issahhanyan, P. Liblik, Phys. Status Solidi C 4 (2007) 1084.
[33] A. Lushchik, Ch. Lushchik, K. Schwartz, F. Savikhin, E. Shablonin, A. Shugai, and E. Vasil'chenko, Nucl. Instrum. Methods B, submitted for publication.
[34] A. Lushchik, Ch. Lushchik, N. Lushchik, A. Frorip, O. Nikiforova, Phys. Status Solidi B 168 (1991) 413.
[35] E.A. Kotomin, A.I. Popov, in: K.E. Sickafus, E.A. Kotomin, B.P. Uberuaga (Eds.), Radiation Effects in Solids, Springer, Amsterdam, 2007 (Chapter 7).
[36] Yu.M. Annenkov, A.M. Pritulov, Fiz. Tverd. Tela 23 (1981) 1065 (Sov. Phys. Solid State 23 (1981) 616).
[37] A. Lushchik, E. Feldbach, S. Galajev, T. Kärner, P. Liblik, Ch. Lushchik, A. Maaroos, V. Nagirnyi, E. Vasil'chenko, Radiat. Meas. 42 (2007) 792.
[38] L.E. Halliburton, L.A. Kappers, Solid State Commun. 26 (1978) 111.
[39] T. Kärner, S. Dolgov, A. Lushchik, N. Mironova-Uulmane, S. Nakonechnyi, E. Vasil'chenko, Radiat. Eff. Defects Solids 155 (2001) 171.
[40] S.A. Dolgov, V. Isakhanyan, T. Kärner, A. Maaroos, S. Nakonechnyi, J. Phys.: Condens. Matter. 15 (2003) 6871.
[41] E.A. Vasil'chenko, N.E. Lushchik, Ch.B. Lushchik, Fiz. Tverd. Tela 12 (1970) 211 (Sov. Phys. Solid State 12 (1970) 167).
[42] M. Kirm, G. Stryganyuk, S. Vielhauer, G. Zimmerer, V.N. Makhov, B.Z. Malkin, O.V. Solovyev, R.Yu. Abdulsabirov, S.L. Korableva, Phys. Rev. B 75 (2007) 075111.
[43] M. Nikl, A. Vedda, M. Fasoli, I. Fontana, V.V. Laguta, E. Mihokova, J. Pejchal, J. Rosa, K. Nejezchleb, Phys. Rev. B 76 (2007) 195121.
[44] K. Blazek, A. Krasnikov, K. Nejezchleb, M. Nikl, T. Savikhina, S. Zazubovich, Phys. Status Solidi B 241 (2004) 1134.
[45] V. Babin, K. Blazek, A. Krasnikov, K. Nejezcheb, M. Nikl, T. Savikhina, S. Zazubovich, Phys. Status Solidi C 2 (2005) 97.
[46] V. Babin, V. Gorbenko, A. Makhov, J.A. Mares, M. Nikl, S. Zazubovich, Yu. Zorenko, J. Lumin. 127 (2007) 384.
[47] V. Mürk, A. Kuznetsov, B. Namozov, K. Ismailov, Nucl. Instrum. Methods B 91 (1994) 327.
[48] M. Kirm, G. Zimmerer, E. Feldbach, A. Lushchik, Ch. Lushchik, F. Savikhin, Phys. Rev. B 60 (1999) 502.
[49] O.F. Schirmer, J. Phys.: Condens. Matter 18 (2006) R667.
[50] J. Devreese, A. Kunz, T. Collins, Solid. State Commun. 11 (1972) 673.
[51] A.M. Stoneham, J. Gavartin, A.L. Shluger, A.V. Kimmel, D. Munoz Ramo, G. Aeppli, C. Renner, J. Phys.: Condens. Matter 19 (2007) 255208.
[52] R.I. Eglitis, E.A. Kotomin, G. Borstel, J. Phys.: Condens. Matter 14 (2002) 3735.
[53] V.M. Tuchkevich, K.K. Schwartz (Eds.), Defects in Insulating Materials, Zinatne, Riga, 1981.
[54] A. Lushchik, I. Tale, S. Zazubovich (Eds.), Proc. 15th Intern. Conf. Defects in Insulating Materials (ICDIM-2004), Wiley-VCH, New York, 2005 (Phys. Status Solidi A 202 (2005) 177–260; Phys. Status Solidi 2 (2005) 15–724).
[55] A. Lushchik, E. Feldbach, R. Kink, Ch. Lushchik, M. Kirm, I. Artinson, Phys. Rev. B 53 (1996) 5379.
[56] N. Ichimura, T. Kawai, S. Hashimoto, Phys. Rev. B 75 (2007) 155121.
[57] K. Tanimura, N. Itoh, Phys. Rev. Lett. 64 (1990) 1429.
[58] T. Tsujibayashi, K. Toyoda, T. Hayashi, Phys. Rev. B 53 (1996) R16129.
[59] A. Lushchik, Ch. Lushchik, K. Schwartz, E. Vasil'chenko, T. Kärner, I. Kudryavtseva, V. Isakhanyan, A. Shugai, Nucl. Instrum. Methods B 266 (2008) 2868.
[60] M. Kirm, A. Lushchik, Ch. Lushchik, Phys. Status Solidi A 202 (2005) 213.
[61] M.K. Kuklja, J. Phys.: Condens. Matter 12 (2000) 2953.
[62] V. Mürk, N. Jaroshevich, Phys. Status Solidi B 181 (1994) K37.